

Expression Profile of Three Splicing Factors in Pleural Cells Based on the Underlying Etiology and Its Clinical Values in Patients with Pleural Effusion



A-Lum Han^{*,1}, Hak-Ryul Kim^{†,1}, Keum-Ha Choi[‡], Jae-won Ryu[§], Ki-Eun Hwang[†], Hong-Seob So[¶], Min-Cheol Park[#], Mengyu Zhu^{**}, Yuya Huang^{**}, Young-Jin Lee^{**} and Do-Sim Park^{**,††,‡‡}

*Department of Family Medicine, School of Medicine, Wonkwang University, Iksan, 54538, Korea; †Department of Internal Medicine, School of Medicine, Wonkwang University, Iksan, 54538, Korea; ‡Department of Pathology, School of Medicine, Wonkwang University, Iksan, 54538, Korea; §School of Medicine, Catholic University of Daegu, Daegu 42472, Korea; ¶Department of Microbiology, School of Medicine, Wonkwang University, Iksan, 54538, Korea; #Department of Oriental Medical Ophthalmology & Otolaryngology & Dermatology, College of Oriental Medicine, Wonkwang University, Iksan, 54538, Korea; **Department of Laboratory Medicine, School of Medicine, Wonkwang University, Iksan, 54538, Korea; ††Wonkwang Institute of Clinical Medicine, Wonkwang University Hospital, Iksan, 54538, Korea; ‡‡Institute of Wonkwang Medical Science, School of Medicine, Wonkwang University, Iksan, 54538, Korea

Abstract

Splicing factors (SFs) are involved in oncogenesis or immune modulation, the common underlying processes giving rise to pleural effusion (PE). The expression profiles of three SFs (HNRNPA1, SRSF1, and SRSF3) and their clinical values have never been assessed in PE. The three SFs (in pellets of PE) and conventional tumor markers were analyzed using PE samples in patients with PE ($N = 336$). The sum of higher-molecular weight (Mw) forms of HNRNPA1 (Sum-HMws-HNRNPA1) and SRSF1 (Sum-HMws-SRSF1) and SRSF3 levels were upregulated in malignant PE (MPE) compared to benign PE (BPE); they were highest in cytology-positive MPE, followed by tuberculous PE and parapneumonic PE. Meanwhile, the lowest-Mw HNRNPA1 (LMw-HNRNPA1) and SRSF1 (LMw-SRSF1) levels were not upregulated in MPE. Sum-HMws-HNRNPA1, Sum-HMws-SRSF1, and SRSF3, but neither LMw-HNRNPA1 nor LMw-SRSF1, showed positive correlations with cancer cell percentages in MPE. The detection accuracy for MPE was high in the order of carcinoembryonic antigen (CEA, 85%), Sum-HMws-HNRNPA1 (76%), Sum-HMws-SRSF1 (68%), SRSF3, cytokeratin-19 fragments (CYFRA 21-1), LMw-HNRNPA1, and LMw-SRSF1. Sum-HMws-HNRNPA1 detected more than half of the MPE cases that were undetected by cytology and CEA. Sum-HMws-HNRNPA1, but not other SFs or conventional tumor markers, showed an association with longer overall survival among patients with MPE receiving chemotherapy. Our results demonstrated different levels of the three SFs with their Mw-specific profiles depending on the etiology of PE. We suggest that Sum-HMws-HNRNPA1 is a supplementary diagnostic marker for MPE and a favorable prognostic indicator for patients with MPE receiving chemotherapy.

Translational Oncology (2018) 11, 147–156

Address all correspondence to: Do-Sim Park, MD, PhD, Department of Laboratory Medicine, Wonkwang University Hospital, 895 Muwang-ro, Iksan 54538, Republic of Korea.

E-mail: emailds@hanmail.net

¹ A. L. H. and H. R. K. are equally contributed.

Received 1 November 2017; Accepted 7 December 2017

© 2017 The Authors. Published by Elsevier Inc. on behalf of Neoplasia Press, Inc. This is an open access article under the CC BY-NC-ND license (<http://creativecommons.org/licenses/by-nc-nd/4.0/>).

1936-5233/18

<https://doi.org/10.1016/j.tranon.2017.12.005>

Introduction

Alternative splicing increases the diversity of the proteome and plays a pivotal role in regulating protein function. The splicing regulatory network has emerged as a critical component of oncogenesis [1] and has impacted many immunologically relevant genes that undergo alternative splicing systems [2–7].

Classical/canonical heterogeneous nuclear ribonucleoproteins (hnRNPs) and serine/arginine-rich (SR) proteins are major classes of nonspliceosomal RNA-binding proteins and have shown multiple splice regulatory functions in splice-site selection and activity [1,8–11]. HNRNPA1, a trans-acting splicing factor (SF) and one of the most abundant and ubiquitously expressed members of the hnRNPs family, is reportedly a splicing silencer for certain exons [8]. SR splicing factor 1 (SRSF1) and SRSF3—members of the SR protein family—have shown several opposite effects to HNRNPA1 [1,4,8–11], including the alternative splicing of CD6, a potential therapeutic target molecule of immune diseases [12]. Regardless of the functional differences among HNRNPA1 and the two SRSFs (SRSF1 and SRSF3) in splicing regulation and diverse expression upon immune cell activation [4,8–11], all these proteins are known as pro-oncotic proteins [1,8,13]. Expressions of the three SFs are frequently deregulated in terms of total amount but also in isoform distribution in various pathophysiologic states, including neoplastic or immune diseases [1,8,11,13–18].

Pleural effusion (PE) is a common, very serious, and potentially fatal medical problem [19]. Malignancy, bacterial pneumonia, and tuberculosis (TB) are common etiologic diseases of PE [19,20]. Etiology identification is crucial for choosing the appropriate therapeutic approach to managing the three types of PE. However, conventional methods are not always capable of establishing the etiology of PE, so alternative tests are needed [19,20].

TB is a representative infectious disease that induces delayed hypersensitivity (a cell-mediated immune response) [21–24]. The development and progression of the other two etiologic diseases of PE

also involve host immune responses [24–28]. In terms of oncogenesis and immune activation, causes of malignant PE (MPE), tuberculous PE (TBPE), and parapneumonic PE (PNPE) share pathophysiologic processes that frequently accompany modified alternative splicing in cells [1–5]. Still, studies that measure the levels of HNRNPA1, SRSF1, and SRSF3 in primary PE cells are hard to find.

These elicit the question of whether the expression profiles of the three SFs in PE samples differ between malignancy and infection-associated host responses. If they differ, then the next questions are whether they are plausible diagnostic markers or prognostic markers in patients with PE, which is best among them from the perspective of efficacy, and whether they are superior to or complementary to currently used tumor markers. To answer these questions, we analyzed the expressions of the three SFs in PE cells and evaluated their detection accuracies (DAs) and prognostic values for MPE in patients with PE and compared the results with the values of conventional tumor markers in supernatant of PE samples.

Materials and Methods

Subjects and Sample Preparation

In total, 336 cellular pellets of PE samples were obtained from 336 Korean patients who had undergone pleural thoracentesis (Table 1). Among these, 131 consecutive patients with MPE who were evaluable in follow-up data were included in the overall survival (OS) analysis. This study was approved by the Institutional Review Board for human studies at Wonkwang University Hospital (No. WKUH 1485). All patients provided written informed consent.

Definitive diagnoses of PE were given by two pulmonologists through independent reviews of the clinical information and pathologic findings. PEs were diagnosed as follows: MPE was diagnosed if cancer cells were detected in the initial cytology, the pleural biopsy histological examination, or upon additional follow-up cell cytology within the admission period without any alternative

Table 1. Characteristics of Patients with PE

Total (N = 336)	MPE (N = 142)			BPE (N = 194)
	Defined (Positive*)	Undefined (Equivocal or Discrepant †)	Missed (Negative ‡)	Defined (Negative)
Age (year), mean ± SD	70 ± 11	70 ± 12	68 ± 14	70 ± 13
Gender, N (%)	46 (65)	23 (53)	20 (63)	140 (72)
Malignant, N	70	40	32	
Lung cancer, N	64	32	15	
ADC, N	51	17	9	–
SQC, N	2	5	3	–
SCLC, N	11	10	3	–
Breast cancer, N	1	1	3	–
Ovary cancer, N	2	1	0	–
Lymphoma, leukemia, N	1	1	4	–
GI cancer, N	0	2	3	–
Other malignancy, N	2	3	7	–
Benign, N				194
Tuberculosis, N	–	–	–	63
Pneumonia, N	–	–	–	88
Cardiovascular and miscellaneous §, N	–	–	–	43

SD, standard deviation; ADC, adenocarcinoma; SQC, squamous cell carcinoma; SCLC, small cell lung cancer; GI, gastrointestinal.

* Positive cytology findings by both pathologists.

† Either equivocal findings by both pathologists or discrepant findings between them.

‡ Negative cytology findings by both pathologists.

§ Cardiovascular disease/surgery with and without renal failure (N = 18), pneumothorax or/and trauma (N = 10), pancreatitis or/and abdominal surgery (N = 9), renal failure with and without liver disease (N = 4), and parasite infection (N = 2).

explanation for exudative PE [19]. TBPE was diagnosed by a positive culture of *Mycobacterium tuberculosis* in the sputum and/or PE, tissue, or caseating granulomas upon a pleural biopsy with compatible clinical findings, or lymphocytic exudative PE with a high adenosine deaminase level and resolved PE in response to an anti-TB treatment and without any alternative explanation for exudative PE [22]. PNPE was diagnosed based on the presence of pulmonary infections associated with acute febrile illness, pulmonary infiltrates, purulent sputum, and the response to an antibiotic treatment or the identification of the organism in the pleural fluid [19]. Other types of BPE were diagnosed by the presence of compatible clinical status without any evidence of TB, malignancy, or current bacterial pneumonia. The functional status of cancer patients was quantified using the Eastern Cooperative Oncology Group (ECOG) scale of performance status (PS) [29].

Sample Preparation

Initial cytology was performed with two equivalently aliquoted samples as routine clinical tests at Wonkwang University Hospital (Iksan, Korea). One aliquot of the sample was stained with Papanicolaou method, and the other was stained with Diff-Quik. The two cytology slides were each examined by two pathologists. The results were classified as follows: 1) positive cytology findings by both pathologists (PC); 2) equivocal findings by both pathologists or discrepant cytology findings between the two pathologists (EC); 3) negative cytology findings by both pathologists (NC). The percentage of cancer cells of an MPE case was determined using the mean number of cancer cells per number of nucleated cells on the two cytology slides that were each counted by two pathologists. If cancer cells were detected on a cytology sample slide and the percentage of cancer cells was equal to or less than 0.01%, the percentage of cancer cells was deemed 0.01%.

A cellular pellet was obtained from each PE sample by acquiring leftover PE samples after routine cytology tests. Red blood cells in the pellets were lysed with ACK lysis buffer (0.5 M NH₄Cl, 10 mM KHCO₃, and 0.1 nM Na₂EDTA at pH 7.2) within 24 hours after the PE sample collection step. The cellular pellets were washed twice with physiologic saline and then were stored frozen in liquid nitrogen until immunoblot analysis.

Immunoblot and Semiquantitative Analysis for SF Proteins

Cellular pellets of PE samples were lysed in RIPA buffer containing protease inhibitors, and the whole-cell lysate was obtained by sequential centrifugation. The proteins were separated on 10% sodium dodecyl sulfate–polyacrylamide gels and then transferred onto polyvinylidene difluoride membranes. The membranes were blocked with 5% skim milk in Tris-buffered saline containing 0.1% Tween 20 (TBS-T), rinsed, and incubated with the appropriate antibodies in TBS-T containing 3% skim milk. The following primary antibodies were used in the immunoblot analysis: anti-HNRNPA1, anti-SRSF1, and anti-SRSF3 (Sigma-Aldrich, St. Louis, MO). Excess primary antibody was then removed by washing the membrane four times in TBS-T. The membranes were then incubated with horseradish peroxidase–conjugated secondary antibody (anti-rabbit or anti-mouse). After three washes in TBS-T, bands were visualized using Clarity Western ECL substrate (Biorad, Hercules, CA) on the FluorChem E system (Protein Simple, Santa Clara, CA).

The optical density of each target molecular weight (Mw) ($\pm 10\%$) region was analyzed with ImageJ software (<http://imagej.nih.gov/ij/>).

The relative levels of respective proteins in the samples were determined after normalization to the total protein level and calibrated using bands from study-defined standard samples [a protein mixture derived from A549 (a non-small cell lung cancer cell line) cells and cellular pellets of PE samples] on each membrane. The total protein level was analyzed using a Hitachi 7600 automatic chemistry analyzer (Hitachi, Tokyo, Japan) and confirmed using Coomassie blue stain band intensity levels. Since HNRNPA1 and SRSF1 showed multiple isoform bands including three intense bands in target areas, each target area was divided into three subareas corresponding to the three intense bands, as shown in Figure 1A (the areas denoted by two orange arrows and one blue arrow, respectively). The value 10 was assigned to the study-defined standard sample, and 0.3 was assigned to undetected bands in the target regions.

Quantitation for Carcinoembryonic Antigen (CEA) and Cytokeratin-19 Fragments (CYFRA 21-1) in PE Samples

CEA and CYFRA 21-1 are commonly used tumor markers in clinical practice [20]. To compare the diagnostic and prognostic values of the SF proteins and tumor markers, the CEA (Immulite 2000; Diagnostic Products Corp., Los Angeles, CA) and CYFRA 21-1 (Cobas e601; Roche Diagnostics, Mannheim, Germany) levels in the supernatant of PE samples were analyzed using chemiluminescence enzyme and electrochemiluminescence immunoassays on automatic analyzers, respectively.

Statistical Analysis

Group values were compared using the Mann-Whitney *U* test (between two groups) or Kruskal-Wallis test (among more than two groups). If values differed significantly in the Kruskal-Wallis test, Conover's *post hoc* tests were performed. Relationships between cancer cell percentages in MPE cases and levels of the SFs or conventional tumor markers were assessed using Spearman correlations. For discriminating between MPE and BPE samples, the DA of each protein was obtained by constructing receiver operating characteristic (ROC) curves. Cutoffs for test positivity were determined by the highest corresponding Youden indexes. Statistical differences in the DAs were analyzed by comparing the areas under independent ROC curves. Statistical differences between the DAs were determined using the DeLong method. Differences in additive detection rates were analyzed with the one-proportion *Z* test. Univariate analysis was performed using Kaplan-Meier and log-rank tests, and multivariate analysis was performed with the Cox proportional hazard model with stepwise selection. Data were analyzed with MedCalc version 17.9.5 (MedCalc Software, Mariakerke, Belgium). Values for which $P < .05$ were considered significant.

Results

Distribution of SF Isoforms in MPE and BPE Samples and Their Relationship with Cancer Cell Fractions in MPE Cases

In the analysis of relative immunoblot band intensity for the SF proteins (Figure 1, A and B), as reported in the introduction by the antibody manufacturer or in previous studies of HNRNPA1 and SRSF1 [6,14,18], HNRNPA1 and SRSF1 proteins of PE samples appeared as multiple isoforms with different electromobilities (Figure 1A). The higher-Mw forms of HNRNPA1 (HMws-HNRNPA1) and SRSF1 (HMws-SRSF1) in each target area (>34 - 36 kDa and >30 - 34 kDa; the areas denoted by the orange arrows in Figure 1A) were

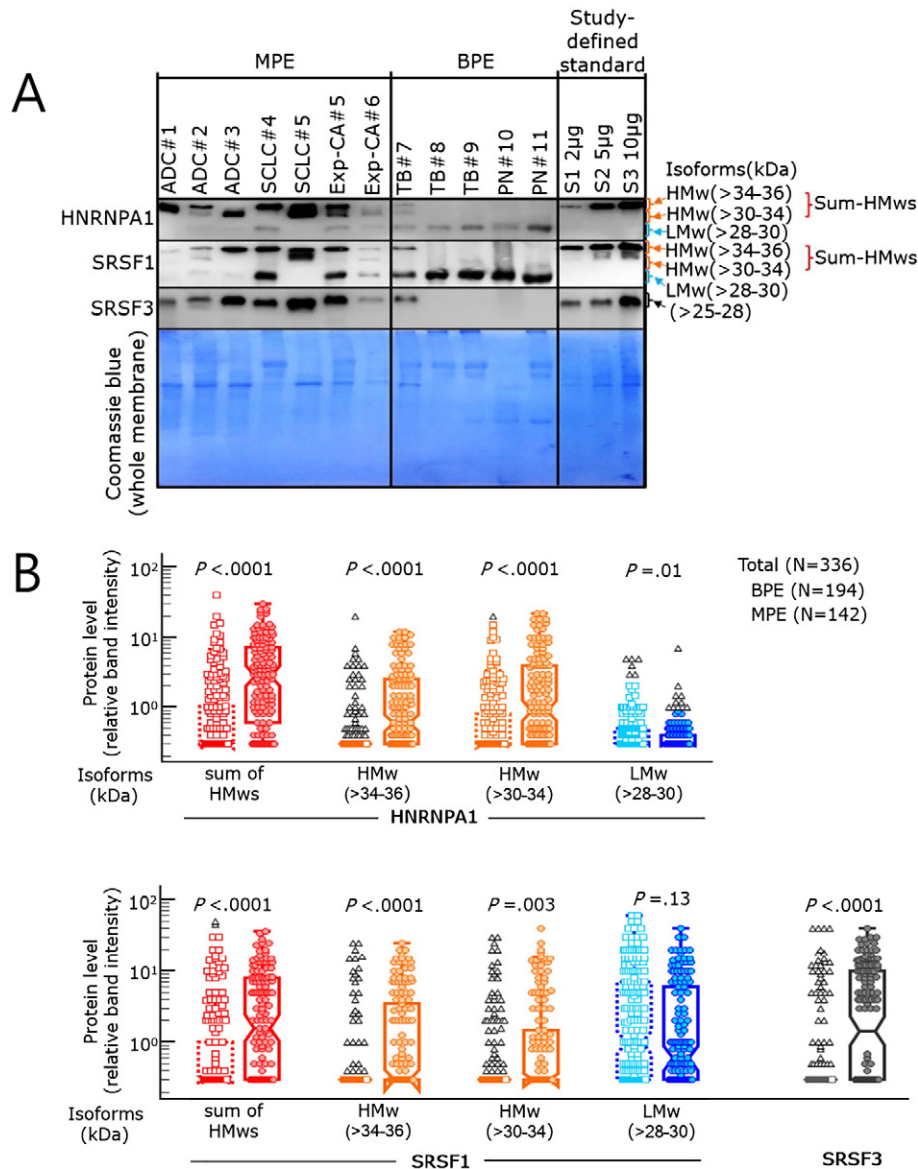


Figure 1. Expression of the three splicing factor proteins in cellular pellet from PE samples. (A) A representative relative immunoblot band intensity analysis in MPE and BPE samples. The Coomassie blue–stained polyvinylidene difluoride membrane was used to confirm the protein loading quantity. The study-defined standard cell lysate (~20 μ g of protein mixture derived from adenocarcinoma cells and cellular pellets of PE) was loaded as a semiquantitative calibrator (S1, S2, and S3). The two orange arrows and one blue arrow indicate individual isoform distinctions according to the Mw of HNRNPA1 and SRSF1, respectively. (B) Comparison of HNRNPA1 and SRSF1 isoforms and SRSF3 levels in semiquantitative immunoblot analysis of MPE (solid lines) and BPE (dotted lines) samples. In the notched box-and-whisker plot, each box and the line inside the box represent the interquartile range and the median; whiskers represent the full range of values excluding outliers (< lower quartile minus 1.5 times the interquartile range or > upper quartile plus 1.5 times the interquartile range); extreme outliers (< lower quartile minus 3.0 times the interquartile range or > upper quartile plus 3.0 times the interquartile range) are plotted as individual triangular points beyond the whiskers. P values were acquired using the Mann-Whitney U test. ADC, adenocarcinoma of lung; SCLC, small cell lung cancer; Exp-CA, extrapulmonary cancer; TB, tuberculosis; PN, pneumonia, kDa, kilodalton; HMw, higher–molecular weight form (>30 kDa, the areas indicated by the orange arrow); Sum-HMws, sum of higher–molecular weight forms; LMw, lowest–molecular weight form (<30 kDa, the areas indicated by the blue arrow).

predominantly detected in MPE samples. When comparing the relative band intensities of MPE and BPE samples, HMw-HNRNPA1 in the >34- to 36-kDa area, HMw-HNRNPA1 in the >30- to 34-kDa area, and their sum (Sum-HMws-HNRNPA1) were significantly higher in MPE samples than BPE samples ($P < .05$, Figure 1B). Notably, the differences between MPE and BPE samples were greater in Sum-HMws-HNRNPA1 than in its individual elements. Specifically, the median level difference (9.3-fold) of Sum-HMws-HNRNPA1

between MPE and BPE samples was far greater than those of HMw-HNRNPA1 in >34-36 kDa (three-fold) or HMw-HNRNPA1 in >30-34 kDa (two-fold). Similar results were obtained for the relative band intensity comparisons between MPE and BPE samples in HMw-SRSF1 in >34-36 kDa, HMw-SRSF1 in >30-34 kDa, and their sum (Sum-HMws-SRSF1). Sum-HMws-SRSF1 and its two individual elements were all higher in MPE samples than in BPE samples, and the median level difference between the MPE and BPE samples of

Sum-HMws-SRSF1 (5.3-fold) was greater than those (<two-fold) of the individual elements.

In contrast, the lowest-Mw (<30 kDa) forms of HNRNPA1 and SRSF1 (LMw-HNRNPA1 and LMw-SRSF1; the area denoted by the blue arrow in Figure 1A) presented a different expressive pattern from that of HMw-SFs; they were predominantly detected in BPE samples rather than MPE samples. Upon comparing the relative band intensities in MPE and BPE samples, as predicted in the finding of Figure 1A, LMw-HNRNPA1 or LMw-SRSF1 either was higher ($P < .01$) or tended to be higher ($P = .13$) in BPE samples than in MPE samples (Figure 1B). The median level difference of LMw-HNRNPA1 (one-fold) or LMw-SRSF1 (1.7-fold) between MPE and BPE samples was not as remarkable as that of Sum-HMws-HNRNPA1 or Sum-HMws-SRSF1 between MPE and BPE samples.

SRSF3 protein appeared as the major isoform, as opposed to multiple isoforms, and SRSF3 bands were predominantly detected in MPE samples. SRSF3 levels in MPE samples were significantly higher than in BPE samples.

In the correlation analysis between cancer cell percentages in MPE cases and levels of the SFs or conventional tumor markers, levels of Sum-HMws-HNRNPA1 and its two elements, Sum-HMws-SRSF1 and its single element (HMw-SRSF1 in >34-36 kDa), SRSF3, and two conventional tumor markers showed a positive correlation ($P < .05$) with cancer cell percentages in MPE cases. HMw-SRSF1 levels in >30-34 kDa did not show any significant relationship with cancer cell percentages in MPE cases ($P > .05$), whereas LMw-HNRNPA1 ($r = -0.17, P = .046$) and LMw-SRSF1 ($r = -0.18, P = .03$) levels

showed a weak negative relationship with cancer cell percentages in MPE cases. Among the SFs and conventional tumor markers, Sum-HMws-HNRNPA1 ($r = 0.42, P < .0001$) and CYFRA 21-1 ($r = 0.36, P < .0001$) showed the strongest and second strongest positive relationships with the cancer cell percentages, respectively.

Levels of the Three SFs in MPE and BPE Sample Subtypes

In the subtype comparison of MPE and BPE samples (Figure 2), Sum-HMws-HNRNPA1 and its two elements, Sum-HMws-SRSF1 and its single element (HMw-SRSF1 in >34-36 kDa), and SRSF3 levels showed the following three key features: 1) they were higher in MPE with PC samples than in all respective BPE subtype samples; 2) in MPE subtype comparison, they were higher in MPE with PC samples than in MPE with NC samples; 3) in BPE subtype comparison, they were significantly higher in TBPE samples than in PNPE samples and were higher or tended to be higher in TBPE samples than in cardiovascular and miscellaneous subtypes of BPE samples (Figure 2). Although trends close to the first and third key features noted in the subtype PE comparisons of Sum-HMws-SRSF1 levels were observed in those of HMw-SRSF1 levels in >30-34 kDa, the second key feature was not observed in subtype PE comparisons of HMw-SRSF1 levels in >30-34 kDa (HMw-SRSF1 levels in >30-34 kDa did not significantly differ between MPE with PC and MPE with NC samples).

As shown by the blue notched box-and-whisker plot in Figure 2, LMw-HNRNPA1 and LMw-SRSF1 presented different expressive patterns from their corresponding HMw-isoforms. They did not

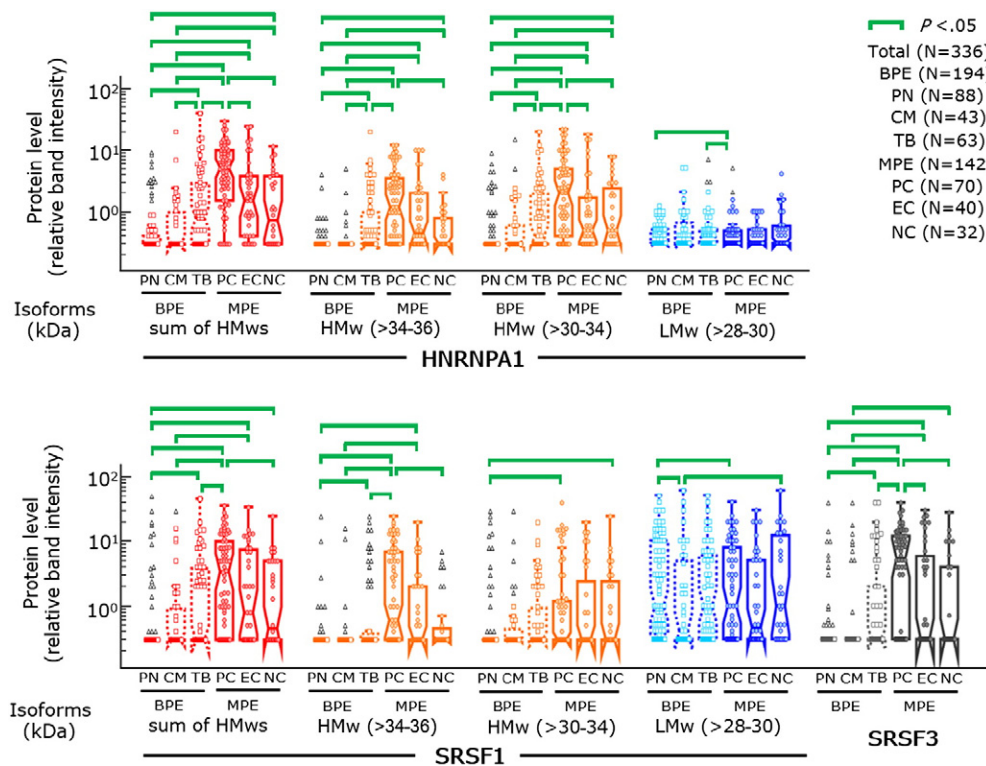


Figure 2. Levels of the three splicing factors in subtypes of MPE and BPE samples. In the notched box-and-whisker plot, each box and the line inside the box represent the interquartile range and the median; whiskers represent the full range of values excluding outliers (< lower quartile minus 1.5 times the interquartile range or > upper quartile plus 1.5 times the interquartile range); extreme outliers (< lower quartile minus 3.0 times the interquartile range or > upper quartile plus 3.0 times the interquartile range) are plotted as individual triangular points beyond the whiskers. P values were acquired using Conover's *post hoc* tests following rejection of a Kruskal-Wallis test among the six subtypes. The green brackets were drawn in the comparisons where P values were less than .05. *CM*, cardiovascular and miscellaneous.

Table 2. Concurrent Comparison of the Detection Accuracy of Splicing Factors and Conventional Tumor Markers for MPE Cases

	Detection Accuracy (95% CI) *, [Sensitivity, %/Specificity, %] [†]	
	MPE (N = 142) vs BPE (N = 194)	MPE with PC (N = 70) vs BPE (N = 194)
Sum-HMws-HNRNPA1	0.76 (0.71-0.80) ^{‡,§} , [75/67]	0.84 (0.79-0.88) [‡] , [83/75]
HMw-HNRNPA1 in >34-36 kDa	0.71 (0.66-0.76) ^{‡,§,} , [62/76]	0.77 (0.712-0.82) ^{§,} , [63/85]
HMw-HNRNPA1 in >30-34 kDa	0.70 (0.64-0.74) ^{§,} , [69/65]	0.75 (0.70-0.80) ^{§,} , [77/65]
LMw-HNRNPA1	0.57 (0.52-0.63) ^{§,} , [65/49]	0.62 (0.56-0.68) ^{‡,§,} , [73/49]
Sum-HMws-SRSF1	0.68 (0.63-0.73) ^{§,} , [63/72]	0.73 (0.67-0.78) ^{§,} , [73/72]
HMw-SRSF1 in >34-36 kDa	0.65 (0.60-0.70) ^{§,} , [44/87]	0.71 (0.65-0.76) ^{§,} , [54/87]
HMw-SRSF1 in >30-34 kDa	0.58 (0.52-0.63) ^{§,} , [35/81]	0.58 (0.51-0.64) ^{‡,§,} , [36/81]
LMw-SRSF1	0.55 (0.49-0.60) ^{‡,§,} , [67/45]	0.59 (0.53-0.65) ^{‡,§,} , [70/45]
SRSF3	0.66 (0.61-0.71) ^{§,} , [50/84]	0.73 (0.68-0.79) ^{§,} , [64/84]
CEA	0.85 (0.80-0.88) ^{‡,} , [70/91]	0.86 (0.81-0.90) [‡] , [71/92]
CYFRA 21-1	0.63 (0.58-0.68) ^{§,} , [61/59]	0.72 (0.66-0.77) ^{§,} , [87/47]

CI, confidence interval.

* Detection accuracy was acquired from the value of the area under the ROC curve by constructing ROC curves.

[†] The cutoffs of SFs and conventional tumor markers were determined by the highest Youden index.

[‡] $P < .05$, compared with CYFRA21-1 (paired area under the curve comparison by the DeLong test).

[§] $P < .05$, compared with CEA (paired area under the curve comparison by the DeLong test).

^{||} $P < .05$, compared with Sum-HMws-HNRNPA1 (paired area under the curve comparison by the DeLong test).

show the three key features that were found in subtype PE comparisons of Sum-HMws-HNRNPA1 and Sum-HMws-SRSF1 levels: 1) LMw-HNRNPA1 and LMw-SRSF1 levels were not significantly higher in MPE with PC samples than in any BPE subtype samples. Instead, they were higher or tended to be higher in the two BPE subtype samples (TBPE and PNPE), which are associated with infection. 2) In MPE subtype comparison, they were not higher in MPE with PC samples than in MPE with NC samples. 3) In BPE subtype comparison, they were not higher in TBPE samples than in PNPE samples.

DA of the Three SFs and Conventional Tumor Markers

In the DA analysis of the three SFs for total MPE samples (Table 2), only Sum-HMws-HNRNPA1 (76%) and HMw-HNRNPA1 in >34-36 kDa (71%) showed acceptable DA (>70%) among all SFs, including the two LMw-SFs (~57%). The DA of Sum-HMws-HNRNPA1 was superior to that (63%) of CYFRA 21-1 (even though CYFRA 21-1 is a currently used tumor marker, it showed an unacceptable DA for MPE samples) but inferior to that (85%) of CEA. While the MPE samples were limited to those with positive cytology findings, Sum-HMws-HNRNPA1 and its two elements, Sum-HMws-SRSF1 and its single element (HMw-SRSF1 in >34-36 kDa), and SRSF3 levels showed acceptable DA (Table 2). Sum-HMws-HNRNPA1 showed the best DA (84%) for MPE with PC samples among all SFs. Moreover, the DA of Sum-HMws-HNRNPA1 was superior to that (72%) of CYFRA 21-1 and comparable to that (86%) of CEA.

Complementary Value of SFs with Acceptable DA and CYFRA 21-1 for Cytology or/and CEA Tests

Additive MPE detection rates were analyzed for cytology-missed/undefined or/and CEA-missed MPE cases to determine whether the SFs with clinically acceptable DA have a complementary role for cytology or/and CEA tests as a diagnostic marker (Table 3). In addition, the complementary values were compared to those of CYFRA 21-1.

More than 50% of high rates of additive detection were obtained by the supplemental use of Sum-HMws-HNRNPA1 test for cytology-missed/undefined (MPE with NC or EC) cases (45/72, 63%), CEA-missed MPE cases (31/43, 72%), or both cytology-missed/undefined and CEA-missed MPE cases (13/23, 57%). Correspondingly, additive detection rates of Sum-HMws-HNRNPA1 were remarkably higher or tended to be higher, with a difference of 9%-21%, compared to not only those of HMw-HNRNPA1 but also those of CYFRA 21-1, one of the most frequently used pleural tumor markers.

Relationship Between SFs and OS

In the initial univariate and multivariate analyses (Table 4) of patient characteristics [age, sex, primary tumor site, ECOG scale of PS, previous history of anticancer chemotherapy (Hx-CTx), and receipt of anticancer CTx after study enrollment (Rece-CTx)] and laboratory tests (cytology, the SFs, and two conventional tumor markers), Rece-CTx showed the strongest association with OS in the log-rank test for survival curve comparison and the greatest differences in the hazard of death between the referent and compared groups with the smallest P value ($P < .0001$). None of the laboratory tests were Rece-CTx-independent OS predictors. Therefore, further stratified analyses were performed according to Rece-CTx (Table 5, Figure 3). In the sequential univariate analysis of Rece-CTx patients, Sum-HMws-HNRNPA1 ($P = .01$) with its single element (HMw-HNRNPA1 in >30-34 kDa, $P = .045$) showed statistically significant association with OS. Additional multivariate analysis adjusted with patient characteristics (age, sex, primary tumor site, ECOG scale of PS, and Hx-CTx) for patients who had Rece-CTx revealed that elevated levels (middle and highest tertiles) of Sum-HMws-HNRNPA1 and its single element were significantly associated with longer OS and were independent predictors for OS. However, for the patients who did not have Rece-CTx, none of the laboratory tests showed a statistically significant association with OS in the univariate analysis. Although there was a trend of an association between OS and cytology ($P = .09$) or CYFRA 21-1 ($P = .08$)

Table 3. Additive Detection Rates by Splicing Factors with Clinically Acceptable Detection Accuracy and CYFRA 21-1 for Cytology-Missed/Undefined or/and CEA-Missed MPE Cases

Total MPE Cases (N = 142)*	Sum-HMws-HNRNPA1, N/N (%)	HMw-HNRNPA1 in >34-36 kDa, N/N (%)	CYFRA 21-1, N/N (%)
Cytology-missed [†] /undefined [‡] (N = 72)	45/72 (63) [§]	38/72 (53)	35/72 (49)
CEA-missed [†] (N = 43)	31/43 (72) ^{§,}	24/43 (56)	22/43 (51)
Cytology-missed [†] /undefined [‡] and CEA-missed [†] (N = 23)	13/23 (57)	9/23 (39)	11/23 (48)

* Fifty of 142 cases were detected by both cytology and CEA tests, and 92/142 cases were missed or undefined by cytology or/and CEA tests.

[†] False negative (the cutoffs of SFs and conventional tumor markers were determined by the highest Youden index).

[‡] Either equivocal findings by both pathologists or discrepant findings between them.

[§] P < .05, compared with CYFRA 21-1 (by one-proportion Z test).

^{||} P < .05, compared with HMws-HNRNPA1 in >34-36 kDa (by one-proportion Z test).

approaching significance in the univariate analysis, no laboratory tests, including the two tests, were statistically significant independent predictors for OS.

Discussion

Regardless of the extensive studies of HNRNPA1, SRSF1, and SRSF3 conducted thus far, features of the three SFs in body fluid cells

other than blood remain mostly unknown [1–4,6–18]. To the best of our knowledge, our study demonstrated for the first time Mw-specific expression profiles of the three SFs in PE samples (a type of body fluid cells), their relationship to PE etiology, as well as their clinical values in diagnosis and prognosis prediction for patients with MPE.

Most previous studies regarding tumor versus nontumor comparisons of the three SFs have focused only on their total amount and did not

Table 4. The Relationship Between Overall Survival and Clinical Variables in Patients with MPE

Patients with MPE (N = 131)	mOS (95% CI), Month	Log-Rank P* (Univariate)	HR [†] (95% CI), P [‡] (Multivariate)
Characteristics of patients			
Age			
≥70 vs <70	3.1 (2.1-4.7) vs 4.3 (3.3-7.1)	.04	NI
Gender			
Male vs female	3.1 (2.3-5.0) vs 4.3 (2.8-7.1)	.20	NI
Primary tumor site			
Lung vs other	4.2 (2.8-6.5) vs 3.1 (1.4-4.0)	.03	NI
ECOG scale of PS			
≥2 vs <2	2.6 (1.5-3.6) vs 4.1 (3.5-8.0)	.001	1.5 (1.1-2.3), .03
Hx-CTx			
Hx-CTx vs none	3.5 (2.3-4.7) vs 4.1 (2.7-7.1)	.43	NI
Rece-CTx			
Non-Rece-CTx vs Rece-CTx	1.4 (0.7-2.1) vs 8.4 (5.0-11.5)	<.0001	4.9 (3.1-7.6), <.0001
Laboratory tests			
Cytology			
Missed [‡] /undefined [§] vs positive	3.1 (2.1-4.3) vs 5.0 (3.3-8.9)	.11	NI
Sum-HMws HNRNPA1			
Lowest vs others (tertile)	3.1 (1.6-4.0) vs 5.0 (3.2-7.1)	.006	NI
HMw-HNRNPA1 in >34-36 kDa			
Lowest vs others (tertile)	2.8 (3.6-8.1) vs 4.7 (6.2-10.9)	.13	NI
HMw-HNRNPA1 in >30-34 kDa			
Lowest vs others (tertile)	3.3 (2.3-4.7) vs 4.3 (2.8-6.5)	.09	NI
LMw-HNRNPA1			
Lowest vs others (tertile)	4.2 (2.8-6.5) vs 3.1 (2.1-4.7)	.21	NI
Sum-HMw-SRSF1			
Lowest vs others (tertile)	3.2 (2.0-4.7) vs 4.2 (2.8-6.5)	.22	NI
HMw-SRSF1 in >34-36 kDa			
Lowest vs others (tertile)	3.1 (2.0-4.1) vs 6.1 (3.1-8.4)	.10	NI
HMw-SRSF1 in >30-34 kDa			
Lowest vs others (tertile)	3.5 (2.7-5.0) vs 4.6 (2.5-6.5)	.50	NI
LMw-SRSF1			
Lowest vs others (tertile)	4.1 (2.7-6.6) vs 3.3 (2.5-4.7)	.82	NI
SRSF3			
Lowest vs others (tertile)	2.8 (1.5-3.8) vs 5.0 (3.6-7.1)	.053	NI
CEA			
Lowest vs others (tertile)	4.3 (2.0-6.5) vs 3.5 (2.8-5.0)	.32	NI
CYFRA21-1			
Lowest vs others (tertile)	3.6 (2.0-4.7) vs 3.6 (2.8-6.2)	.42	NI

mOS, median overall survival; HR, hazard ratio for death; NI, not included.

* Univariate analysis was performed using Kaplan-Meier and log-rank tests.

[†] Multivariate analysis was done with the Cox proportional hazard model with stepwise selection (variables with P > .10 were removed in the multivariate model). HR was acquired after adjusting for covariates (age, sex, primary tumor site, ECOG scale of PS, Hx-CTx, and Rece-CTx).

[‡] False negative (the cutoffs of SFs and conventional tumor markers were determined by the highest Youden index).

[§] Either equivocal findings by both pathologists or discrepant findings between them.

Table 5. The Relationship Between Overall Survival and Laboratory Tests According to Receipt of Chemotherapy in Patients with MPE

Patients with MPE (N = 131)	Rece-CTx (N = 76)		None (N = 55)	
	Log-Rank P* (Univariate)	HR (95% CI), P† (Multivariate)	Log-Rank P (Univariate)	HR (95% CI), P‡ (Multivariate)
Cytology				
Missed [§] /undefined [§] vs positive	.63	NI	.09	NI
Sum-HMws HNRNPA1				
Lowest vs others (tertile)	.01	2.0 (1.1-3.5), .02	.30	NI
HMw-HNRNPA1 in >34-36 kDa				
Lowest vs others (tertile)	.23	NI	.40	NI
HMw-HNRNPA1 in >30-34 kDa				
Lowest vs others (tertile)	.045	1.8 (1.1-3.0), .03	.37	NI
LMw-HNRNPA1				
Lowest vs others (tertile)	.12	NI	.73	NI
Sum-HMws-SRSF1				
Lowest vs others (tertile)	.54	NI	.30	NI
HMw-SRSF1 in >34-36 kDa				
Lowest vs others (tertile)	.22	NI	.68	NI
HMw-SRSF1 in >30-34 kDa				
Lowest vs others (tertile)	.56	NI	.41	NI
LMw-SRSF1				
Lowest vs others (tertile)	.87	NI	.82	NI
SRSF3				
Lowest vs others (tertile)	.07	NI	.45	NI
CEA				
Lowest vs others (tertile)	.14	NI	.25	NI
CYFRA21-1				
Lowest vs others (tertile)	.20	NI	.08	NI

* Univariate analysis was performed using Kaplan-Meier and log-rank tests.

† Multivariate analysis was done with the Cox proportional hazard model with stepwise selection (variables with $P > .10$ were removed in the multivariate model); HR was acquired after adjusting for covariates (age, sex, primary tumor site, ECOG scale of performance status, and previous history of anticancer chemotherapy).

§ Either equivocal findings by both pathologists or discrepant cytology findings between them.

include benign inflammatory conditions [13–15]. Unlike those, our MPE versus BPE and their subtype comparison as conducted here demonstrated a remarkable difference between two HMw-SFs and their corresponding LMw-SFs, particularly between the sum of HMw isoforms and their corresponding LMw isoforms. We also evaluated for benign infectious diseases that should be differentiated from malignancy.

In the context of Sum-HMws-HNRNPA1, Sum-HMws-SRSF1, and SRSF3, current findings (their levels were not only higher in MPE samples than in BPE samples but higher in MPE with PC samples than in MPE with NC samples) match the reported roles of the three SFs which promote cellular proliferation or the synthesis of antiapoptotic splice variants [1,8,11,13]. Our comparison results are

consistent with those of previous studies [1,8,11,13] showing relatively upregulated expression of the SFs in lung cancer and breast cancer (which frequently metastasize to the pleural space) samples compared to normal tissue samples and the current correlation relationship between the SFs (Sum-HMws-HNRNPA1, Sum-HMws-SRSF1, and SRSF3) levels and the cancer cell percentages in MPE cases.

Meanwhile, in view of the two LMw-SFs, LMw-HNRNPA1 and LMw-SRSF1 levels were higher or showed a higher tendency in BPE samples than they did in the MPE samples. This is a new finding, which somewhat contradicts the known increased tumor/nontumor ratios for total amount of the two SFs [1,8,11,13]. Although Mw-shifted-HNRNPA1 or -SRSF1 inducing clinical status has rarely been studied, a granzyme (cytotoxic protease upregulated during bacterial infection and released by immune cells)-treated cell line model showed cleavage of HNRNPA1 as a mobility shift (faster migration) on an immunoblot, which is fairly consistent with the relative levels of LMw-HNRNPA1 in PNPE and TBPE [6,30]; these types of PEs are associated with bacterial infection and immune cell activation [21,23–26].

Regarding benign infectious conditions, in the subtype PE comparison between TBPE and PNPE samples, we noted significantly higher levels of Sum-HMws-HNRNPA1, Sum-HMws-SRSF1, and SRSF3 in TBPE samples compared to those in PNPE samples. Few studies have demonstrated SRSF1-enhanced production of certain cytokines including type-1 interferons (INFs) [31]. A local immune deviation of PE showed a remarkable difference between TBPE and PNPE in concentrations of specific cytokines and accumulated immune cell proportion by the PE etiology including pathogens (*Mycobacterium tuberculosis* versus bacteria other than *Mycobacterium* species) [24,32]. For example, the concentration of

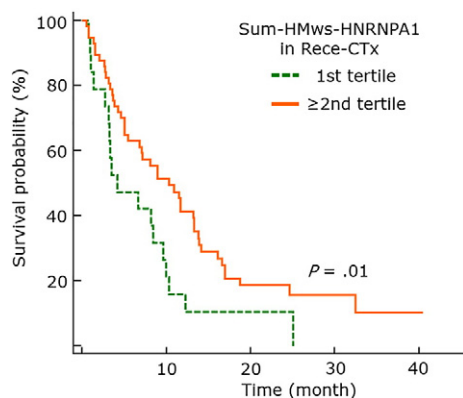


Figure 3. Overall survival difference between the first (lower level) and ≥second (higher level) tertiles of Sum-HMws-HNRNPA1 level in MPE patients who received anticancer chemotherapy after study enrollment (Rece-CTx, N = 76).

INF- γ , a type-1 INF, in TBPE is higher than that in PNPE, and generally, TBPE has a higher proportion of lymphocytes than PNPE [24,32]. Our observation is in line with previous reports [24,32]. Together, these support the possibility that the three SFs are involved in pathogen-specific immune responses. Although we could not pinpoint the mechanism by which this occurs, it can be explained as TB-specific pleural microenvironment [21,23,32] affecting the expressions of the SFs or blood immune cells with higher levels of the SFs (including specific Mw-SF isoforms) which migrate into the pleural space during TB-induced inflammation [32–34].

Despite the significant difference in the SF levels among the BPE subtypes with higher levels of those in TBPE samples than in PNPE samples, the levels of Sum-HMws-HNRNPA1, Sum-HMws-SRSF1, and SRSF3 were much higher in MPE with PC samples than in TBPE samples. This may indicate that cancer cells have relatively higher levels of Sum-HMws-HNRNPA1, Sum-HMws-SRSF1, and SRSF3 than infection-associated immune cells. Alternatively, it may indicate that tumor-associated status, including a tumor antigen-associated immune reaction, is a stronger stimulant of the induction of Sum-HMws-HNRNPA1, Sum-HMws-SRSF1, and SRSF3 than any infection-associated immune responses. Together, these findings indicate that the expression profile of the three SFs in PE samples differ between malignancy and the infection-associated host response, thus addressing the first question of this study.

Through the DA analysis, we demonstrated that Sum-HMws-HNRNPA1, rather than individual elements of Sum-HMws-HNRNPA1 or LMw-HNRNPA1, is the most efficient MPE detection marker among the three SFs. Moreover, Sum-HMws-HNRNPA1, but not LMw-HNRNPA1, showed comparable (CEA) or superior (CYFRA-21) detection efficiency to that of currently used tumor markers for MPE with PC samples. A serologic study has shown a CEA-comparable DA of HNRNPA1 for colon cancer cases [15]. Regarding DA for cancer, our results showed the expanded potential of HNRNPA1 as a pleural marker from its reported potential as a blood marker. Furthermore, noticeable additive detection power and superior additive detection rate of Sum-HMws-HNRNPA1 compared to CYFRA 21-1 (a CEA-complementary pleural tumor marker) for cytology or/and CEA undetected MPE cases support its use as a supplementary diagnostic marker for MPE.

The prognostic implications of the three SFs in cancer patients remain unclear, and two previous studies [16,35] presented somewhat conflicting prognostic relevance for *HNRNPA1* gene and its protein expression. One showed a higher frequency of *HNRNPA1* gene overexpression in low-stage compared to high-stage colon cancer cases [35]. The other found shorter OS in hepatocellular carcinoma patients with elevated HNRNPA1 levels [16]. Our study demonstrated the various prognostic implications of HNRNPA1 depending on its Mw-specific isoforms and patients' use of anticancer CTx. Elevated levels of Sum-HMws-HNRNPA1 with its single element (HMw-HNRNPA1 in >30–34 kDa), but not LMw-HNRNPA1, revealed a role as a favorable prognosis predictor for patients who had Rece-CTx but not for those who did not. This finding is linked to the fact that HNRNPs affect the responses to anticancer CTx, acting as mediators or modulators of drug-induced apoptosis [11], and the prognostic implication of HMw-HNRNPA1 in patients who had Rece-CTx is partly in line with the former study [35]. However, the prognostic implication of HNRNPA1 in the latter study conflicts with that of HMw-HNRNPA1 in our study, specifically for patients who had Rece-CTx. Regarding this disparity, we speculate that

patients' condition and management after the enrolled time are among the major causes [i.e., all of our cases who were treated with CTx had pleural metastasis with unresectable cancer cells (in this unresectable advanced condition, fast-growing, rather than slow-growing, cancer cells may respond well to CTx), and our cases consisted of individuals with different types of nonhepatic cancer versus hepatocellular cancer cases with a localized mass in the liver that was readily resected]. The next plausible cause is the analytical method (immunoblot for total amount of HNRNPA1 versus immunohistochemical staining for total amount of HNRNPA1). Considering the use of anticancer CTx—dependent alteration of prognostic implications for HMw-HNRNPA1 in our study, the patients' statuses are considered more likely to have contributed to the outcomes. Again, the valid relationship between OS and HMw-HNRNPA1 and the OS-related comparison findings for the three SFs and two conventional tumor markers are in response to our final question.

In summary, our results revealed elevated Sum-HMws-HNRNPA1, Sum-HMws-SRSF1, and SRSF3 levels in MPE samples compared to BPE samples, with their additional comparison in subtype PE showing that they were high in the order of MPE with PC, TBPE, and PNPE and that this trend in two HMw-SFs is remarkably different from that of their corresponding LMw-SFs. The findings of DA and OS analysis in the current study suggest the practical application of Sum-HMws-HNRNPA1 as a novel pleural diagnostic and prognostic marker given its CEA-comparable DA, high additive detection power, and significant association between elevated Sum-HMws-HNRNPA1 and longer OS in patients with MPE receiving anticancer CTx.

Conflict of Interest Statement

The authors declare no conflict of interest in relation to this study.

Acknowledgments

A. L. H. and H. R. K. contributed equally. The biospecimens and clinical data used in this study were provided by the members of Korea Biobank Network (Wonkwang University Hospital). This research was supported by the Basic Science Research Program through the National Research Foundation of Korea funded by the Korean government [the Ministry of Education (NFR-2016R1D1A1B04935786) and the Ministry of Science, ICT & Future Planning (NRF-2011-0030130 and NRF-2015M3A9E3051054)].

References

- [1] Shilo A, Siegfried Z, and Karni R (2014). The role of splicing factors in deregulation of alternative splicing during oncogenesis and tumor progression. *Mol Cell Oncol* **2**, e970955.
- [2] Schaub A and Glasmacher E (2017). Splicing in immune cells—mechanistic insights and emerging topics. *Int Immunol* **29**, 173–181.
- [3] Martinez NM and Lynch KW (2013). Control of alternative splicing in immune responses: many regulators, many predictions, much still to learn. *Immunol Rev* **253**, 216–236.
- [4] da Glória VG, Martins de Araújo M, Mafalda Santos A, Leal R, de Almeida SF, Carmo AM, and Moreira A (2014). T cell activation regulates CD6 alternative splicing by transcription dynamics and SRSF1. *J Immunol* **193**, 391–399.
- [5] Rodrigues R, Grosso AR, and Moita L (2013). Genome-wide analysis of alternative splicing during dendritic cell response to a bacterial challenge. *PLoS One* **8**, e61975.
- [6] Rajani DK, Walch M, Martinvalet D, Thomas MP, and Lieberman J (2012). Alterations in RNA processing during immune-mediated programmed cell death. *Proc Natl Acad Sci U S A* **109**, 8688–8693.

- [7] Moulton VR, Gillooly AR, and Tsokos GC (2014). Ubiquitination regulates expression of the serine/arginine-rich splicing factor 1 (SRSF1) in normal and systemic lupus erythematosus (SLE) T cells. *J Biol Chem* **289**, 4126–4134.
- [8] Jean-Philippe J, Paz S, and Caputi M (2013). hnRNP A1: the Swiss army knife of gene expression. *Int J Mol Sci* **14**, 18999–19024.
- [9] Zhu J, Mayeda A, and Krainer AR (2001). Exon identity established through differential antagonism between exonic splicing silencer-bound hnRNP A1 and enhancer-bound SR proteins. *Mol Cell* **8**, 1351–1361.
- [10] Bonomi S, di Matteo A, Buratti E, Cabianca DS, Baralle FE, Ghigna C, and Biamonti G (2013). HnRNP A1 controls a splicing regulatory circuit promoting mesenchymal-to-epithelial transition. *Nucleic Acids Res* **41**, 8665–8679.
- [11] Kędzierska H and Piekietko-Witkowska A (2017). Splicing factors of SR and hnRNP families as regulators of apoptosis in cancer. *Cancer Lett* **396**, 53–65.
- [12] Pinto M and Carmo AM (2013). CD6 as a therapeutic target in autoimmune diseases: successes and challenges. *BioDrugs* **27**, 191–202.
- [13] Jia R, Li C, McCoy JP, Deng CX, and Zheng ZM (2010). SRp20 is a proto-oncogene critical for cell proliferation and tumor induction and maintenance. *Int J Biol Sci* **6**, 806–826.
- [14] David CJ, Chen M, Assanah M, Canoll P, and Manley JL (2010). HnRNP proteins controlled by c-Myc deregulate pyruvate kinase mRNA splicing in cancer. *Nature* **463**, 364–368.
- [15] Ma YL, Peng JY, Zhang P, Huang L, Liu WJ, Shen TY, Chen HQ, Zhou YK, Zhang M, and Chu ZX, et al (2009). Heterogeneous nuclear ribonucleoprotein A1 is identified as a potential biomarker for colorectal cancer based on differential proteomics technology. *J Proteome Res* **8**, 4525–4535.
- [16] Zhou ZJ, Dai Z, Zhou SL, Fu XT, Zhao YM, Shi YH, Zhou J, and Fan J (2013). Overexpression of HnRNP A1 promotes tumor invasion through regulating CD44v6 and indicates poor prognosis for hepatocellular carcinoma. *Int J Cancer* **132**, 1080–1089.
- [17] Naro C and Sette C (2013). Phosphorylation-mediated regulation of alternative splicing in cancer. *Int J Cell Biol* **2013**151839.
- [18] Zou L, Zhang H, Du C, Liu X, Zhu S, Zhang W, Li Z, Gao C, Zhao X, and Mei M, et al (2012). Correlation of SRSF1 and PRMT1 expression with clinical status of pediatric acute lymphoblastic leukemia. *J Hematol Oncol* **5**, 42.
- [19] Daniil ZD, Zintzaras E, Kiroopoulos T, Papaioannou AI, Koutsokera A, Kastanis A, and Gourgoulis KI (2007). Discrimination of exudative pleural effusions based on multiple biological parameters. *Eur Respir J* **30**, 957–964.
- [20] Antonangelo L, Sales RK, Corá AP, Acencio MM, Teixeira LR, and Vargas FS (2015). Pleural fluid tumour markers in malignant pleural effusion with inconclusive cytologic results. *Curr Oncol* **22**, e336–341.
- [21] Brighenti S and Andersson J (2012). Local immune responses in human tuberculosis: learning from the site of infection. *J Infect Dis* **205**, S316–324.
- [22] Ko Y, Kim C, Chang B, Lee SY, Park SY, Mo EK, Hong SJ, Lee MG, Hyun IG, and Park YB (2017). Loculated tuberculous pleural effusion: easily identifiable and clinically useful predictor of positive mycobacterial culture from pleural fluid. *Tuberc Respir Dis* **80**, 35–44.
- [23] Schierloh P, Landoni V, Balboa L, Musella RM, Castagnino J, Moraña E, de Casado GC, Palmero D, and Sasiain MC (2014). Human pleural B-cells regulate IFN- γ production by local T-cells and NK cells in a Mycobacterium tuberculosis-induced delayed hypersensitivity reaction. *Clin Sci* **127**, 391–403.
- [24] Kroegel C and Antony VB (1997). Immunobiology of pleural inflammation: potential implications for pathogenesis, diagnosis and therapy. *Eur Respir J* **10**, 2411–2418.
- [25] Galluzzi L, Buqué A, Kepp O, Zitvogel L, and Kroemer G (2017). Immunogenic cell death in cancer and infectious disease. *Nat Rev Immunol* **17**, 97–111.
- [26] Antony VB (2003). Immunological mechanisms in pleural disease. *Eur Respir J* **21**, 539–544.
- [27] Wurz GT, Kao CJ, Wolf M, and DeGregorio MW (2014). Tecemotide: an antigen-specific cancer immunotherapy. *Hum Vaccin Immunother* **10**, 3383–3393.
- [28] Oshikawa K, Yanagisawa K, Ohno S, Tominaga S, and Sugiyama Y (2002). Expression of ST2 in helper T lymphocytes of malignant pleural effusions. *Am J Respir Crit Care Med* **165**, 1005–1009.
- [29] Oken MM, Creech RH, Tormey DC, Horton J, Davis TE, McFadden ET, and Carbone PP (1982). Toxicity and response criteria of the Eastern Cooperative Oncology Group. *Am J Clin Oncol* **5**, 649–655.
- [30] García-Laorden MI, Stroo I, Terpstra S, Florquin S, Medema JP, van T Veer C, de Vos AF, and van der Poll T (2017). Expression and function of granzymes A and B in Escherichia coli peritonitis and sepsis. *Mediat Inflamm* **2017**4137563.
- [31] Xue F, Li X, Zhao X, Wang L, Liu M, Shi R, and Zheng J (2015). SRSF1 facilitates cytosolic DNA-induced production of type I interferons recognized by RIG-I. *PLoS One* **10**, e0115354.
- [32] Ribera E, Ocaña I, Martínez-Vázquez JM, Rossell M, Español T, and Ruibal A (1988). High level of interferon gamma in tuberculous pleural effusion. *Chest* **93**, 308–311.
- [33] Wu C, Ma J, Xu Y, Zhang X, Lao S, and Yang B (2014). Pleural fluid mononuclear cells (PFMCs) from tuberculous pleurisy can migrate in vitro in response to CXCL10. *Tuberculosis* **94**, 123–130.
- [34] Nasreen N, Mohammed KA, Ward MJ, and Antony VB (1999). Mycobacterium-induced transmesothelial migration of monocytes into pleural space: role of intercellular adhesion molecule-1 in tuberculous pleurisy. *J Infect Dis* **180**, 1616–1623.
- [35] Ushigome M, Ubagai T, Fukuda H, Tsuchiya N, Sugimura T, Takatsuka J, and Nakagama H (2005). Up-regulation of hnRNP A1 gene in sporadic human colorectal cancers. *Int J Oncol* **26**, 635–640.